Journal of Hydroscience and Hydraulic Engineering
Vol. 28, No.1 May, 2010, 117-125

STUDY OF WALL MODEL IN LES CALCULATION OF TURBULENT FLOW OVER COMPLEX BOUNDARY

by

Tomoaki Kasai

Graduate School of Engineering, Kobe University, 1-1 Rokkodai-cho, Nada-ku, Kobe Japan

and

Akihiko Nakayama

Graduate School of Engineering, Kobe University, 1-1 Rokkodai-cho, Nada-ku, Kobe, Japan

SYNOPSIS

A wall stress model for Large-eddy simulations (LES) of flows over complex boundaries that involve flow separation and roughness effects is proposed and verified in a few test cases. It is based on a resistance formula for the bulk flow parameters applied to the near-wall flow on a local and temporal basis and is much simpler than the previous method involving dynamic determination of model constants. The results indicate that the new wall-stress model used in conjunction with the standard Smagorinsky model or the newer shear-improved Smagorinsky model gives consistently good results of the mean velocity and the Reynolds stresses. The grid we used is a very coarse grid and does not resolve the viscous sub-layer or the buffer layer. More commonly used logarithmic-law similarity or the power-law similarity is found to produce incorrect results in the separated or reattaching regions. Since it is impossible to resolve viscous sub-layers in real-scale applications with computational grids that can be accommodated by available computer systems, the proposed model will be useful in such applications. Test calculations also indicate that the standard Smagorinsky sub-grid scale model, which is known to work only if the wall layer is resolved and if damping is applied to the eddy viscosity coefficient in the viscosity dominated region, yields surprisingly good results if no wall model is used at all.

INTRODUCTION

With the ever increasing power of digital computers, Large Eddy Simulation (LES), which was thought to be too costly to perform calculations of real-scale open-channel flows and realistic river flows, is coming within the reach of practical hydraulic engineers (eg. (1, 2)). It gives detailed information of the three-dimensional turbulent motion that is very important in solving various engineering problems such as the estimation of the drag on the bed, transport of sediment and other hydrodynamic forces on structures. The LES method has been tested and validated in basic flows such as homogeneous turbulence and fully-developed channel flows (1, 2) but has not yet been tested in simulation of large-scale flows over complex boundaries. For large-scale flows, the fraction of fluctuating motion that can be resolved compared with the entire flow decreases and the accuracy of the flow simulation depends more on the accuracy of representation of the unresolved modelled part of the flow. Therefore, much focus has been placed on developing accurate and efficient sub-grid scale (SGS) models. However, for realistic flows with complex boundary geometry, not only the SGS stresses but the boundary effects must also be accurately represented. The flow near solid boundaries in real scale flows cannot be resolved to obtain the boundary stress without a model.

'Wall models' have been studied intensively to make the LES applicable to high-Reynolds number engineering flows in which the near-wall flow cannot be resolved (e.g. Piomelli and Balaras (3)), but the problem is still unsolved. Particularly when the boundary geometry becomes complex and rough, no working wall model is available. The present authors proposed (Kitano and Nakayama (4)) a model applicable to arbitrary geometry with un-resolvable roughness by a dynamic procedure, in which the unresolved boundary effects are estimated from the resolved flow and the resolved boundary shape. However, the procedure involves complicated filtering over complex flow field and takes a considerable amount of computational time for practical calculations. The values of the model coefficient thus determined were found to be close to the values implied by conventional resistance formula, which can be exploited to simplify the model.

In the present work, a more simplified model in which the model coefficient that was determined by a dynamic procedure is fixed at a nominal value estimated from the overall resistance of the flow, is proposed and tested in a few different flow conditions. The first test case is a flow over model hills placed at the bottom boundary of a long channel, which has been computed by reliable high-resolution LES by Temmerman, L. and Leschziner (5). The second test case is a wavy surface for which Direct Numerical Simulation (DNS) has been done by the present authors (6). The latter case can also be regarded as a flow over a model rough surface since the height of the waviness is only 5 percent of the channel depth. Two commonly used SGS models are used in conjunction with the present wall model, and the relative merits are

also discussed.

BASIC EQUATIONS, SGS MODELS AND WALL MODELS

Basic equations

The basic equations for the filtered flow field are the filtered equations of motion

$$\frac{\partial u_i}{\partial t}+\frac{\partial u_i u_j}{\partial x_j}=-\frac{1}{\rho}\frac{\partial P}{\partial x_i}+g_i+\frac{\partial}{\partial x_j}\left[\nu\left(\frac{\partial u_i}{\partial x_j}+\frac{\partial u_j}{\partial x_i}\right)+\frac{\tau_{ij}}{\rho}\right] \tag{1}$$

and the filtered continuity equation

$$\frac{\partial u_i}{\partial x_i}=0 \tag{2}$$

for incompressible flows, where u_i is the spatially-filtered velocity component in the Cartesian coordinates x_i, P is the filtered pressure, g_i is the component of the gravitational acceleration in x_i direction, ν is the kinematic viscosity coefficient and τ_{ij} is the subgrid-scale stress. It is noted that we do not use the explicitly filtered form of the equations of motion, which is

$$\frac{\partial u_i}{\partial t}+\frac{\partial\left\langle u_i u_j\right\rangle}{\partial x_j}=-\frac{1}{\rho}\frac{\partial P}{\partial x_i}+g_i+\frac{\partial}{\partial x_j}\left[\nu\left(\frac{\partial u_i}{\partial x_j}+\frac{\partial u_j}{\partial x_i}\right)+\frac{\tau_{ij}}{\rho}+\left(\left\langle u_i u_j\right\rangle-u_i u_j\right)\right] \tag{3}$$

where the angular brackets indicate filtering (saving the overbar to mean the time average) which can be explicitly performed but requires additional definition of the filter and extra computation (7). The implicit form (1) necessarily makes use of the numerical filtering effects is thought more efficient in real-scale applications and used in the present work. The filtered pressure P in Equation (1) includes the isotropic part of the subgrid stress so that τ_{ij} contains only the non-isotropic part which can be expressed by the eddy viscosity model with kinematic eddy viscosity coefficient ν_t as

$$\frac{\tau_{ij}}{\rho}=\nu_t\left(\frac{\partial u_i}{\partial x_j}+\frac{\partial u_j}{\partial x_i}\right) \tag{4}$$

This form does not require an additional model for the isotropic part. The eddy viscosity representation with an appropriately determined eddy viscosity coefficient works well within the flow in most cases. However, near solid walls, particularly if the non-slip wall condition is used and if zero velocity is assumed on the wall, the velocity gradient is significantly underestimated and the wall stress is calculated incorrectly. This is the main difficulty in using Equation (4) near the wall in high Reynolds number flows. We present the wall stress model that circumvents this difficulty in the following section.

SGS models

For the SGS model, we use the commonly used standard Smagorinsky model (8) and the shear-improved Smagorinsky model proposed by Leveque et al. (9) that has been shown to do as well as the dynamic Smagorinsky model without performing a numerical filtering (5). The standard Smagorinsky model with a near wall damping is given by:

$$\nu_t=\left(C_s\Delta\right)^2\left(1-e^{-y^+/25}\right)^2\left(|S|\right) \tag{5}$$

where Cs is the Smagorinsky constant (in the present work, taken as Cs=0.1), Δ is the filter size (in the present work, taken as the geometric average of grid spacings in three directions), $y^+=u_\tau y/\nu$, where y is the distance to the wall and u_τ is the friction velocity, and S is the rate of deformation tensor and

$$|S|=\frac{1}{2}\left|\frac{\partial u_i}{\partial x_j}+\frac{\partial u_j}{\partial x_i}\right| \tag{6}$$

The shear-improved Smagorinsky model has been shown to give good results both in homogeneous and wall turbulence including those transitioning from laminar to turbulent flows (9). It is given by:

$$\nu_t = (C_S \cdot \Delta)^2 \cdot \left(|S| - |\overline{S}|\right) \tag{7}$$

where the overbar indicates the ensemble or time average. In the present validation calculation, since the geometry is two-dimensional, the transverse average is used.

Wall models

In this section we describe the wall models used in the present work including a new simplified one. Wall models relate the local and instantaneous wall shear stress to the velocity near the wall without using the molecular viscosity law. Most of the existing models make use of similarity relations for the velocity distributions near wall expressed in terms of the wall shear stress (eg. Piomelli and Balaras (3)). However, the instantaneous velocity distributions fluctuate around the mean velocity distribution with the amplitude as large as the local turbulence intensity and do not follow the similarity most of the time (Nakayama et al. (10)). Since the resistance coefficient defined for global flow depends little on the Reynolds number if it is sufficiently large, we assume that the local and temporal wall shear stress τ_w is given by a resistance formula based on the local velocity u_1 as

$$\tau_w = \rho C_d u_1 |u_1| \tag{8}$$

where C_d is a resistance coefficient which is in general dependent on the Reynolds number, the local geometry, and the temporal condition, such as acceleration with a sweep-type motion or deceleration, and the way u_1 is chosen (10). It depends almost on the exact equations of motion near the wall, but the experimental data implied that the temporal mode is the most important factor. In a previous work, Vengadesan and Nakayama (11) used the temporal pressure gradient as a parameter in the standard logarithmic-law similarity and found to improve prediction of the flow over curved hills. Kitano and Nakayama(4) determined this resistance coefficient by taking the test filter and assuming scale similarity as is done in dynamic SGS models. The results indicated that the dynamically determined resistance coefficient took values close to the resistance coefficient for the entire channel flow. Furthermore they tend to be constant for higher Reynolds numbers. Based on this, we choose a value that gives the correct overall resistance that is in a similar form as the resistance formula for a flat surface:

$$\sqrt{C_d} = \frac{B}{\log\left(\frac{U_0 \Delta_x}{\nu} C_d\right)} \tag{9}$$

where U_0 is the mean bulk velocity, Δ_x is the grid spacing in the streamwise direction and B is a model constant set at 0.241 same as that used for flat surface boundary layer (12). The main point of the above relation is that U_0 and B are the global values not local as used in most wall models with local similarity, so that the total resistance in the entire channel comes close to that implied by the global resistance formula. Henceforth this will be referred to as WSM model.

The above-described wall model is compared with the more conventional ones given below. First the most-commonly used two-layer model based on the logarithmic law and the linear law applied to the velocity magnitude u_1 at the first calculation point which is y_1 from the wall.

$$\tau_w = \begin{cases} \rho \dfrac{\nu u_1}{y_1}, & \dfrac{\sqrt{\tau_w/\rho}\, y_1}{\nu} \le 10 \\ \dfrac{\rho u_1^2}{\dfrac{1}{\kappa}\left(\ln\left(\dfrac{\sqrt{\tau_w/\rho}\, y_1}{\nu}\right) + A\right)^2}, & \dfrac{\sqrt{\tau_w/\rho}\, y_1}{\nu} > 10 \end{cases} \tag{10}$$

where κ is the von Karman constant and A is the constant in the log law. This will be referred to as LL model.

The next one is based on the linear law and the power law proposed by Werner and Wengle (13). It is given by:

$$\tau_w = \begin{cases} \rho \dfrac{\nu u_1}{y_1}, & \dfrac{\sqrt{\tau_w/\rho}\, y_1}{\nu} \le 11.8 \\ \rho \left(\dfrac{\nu u_1^7}{8.7^7 y_1} \right)^{\frac{1}{4}}, & \dfrac{\sqrt{\tau_w/\rho}\, y_1}{\nu} > 11.8 \end{cases} \tag{11}$$

This is designated by WW. It was used by Temmerman and Leschziner (5) in a calculation of flow over hills and found to give good results. That calculation resolved the viscous sub-layer $\sqrt{\tau_w/\rho}\, y_1 / \nu < 10$, and performance for high Reynolds number flows is not known.

NUMERICAL METHOD

The calculation method used in the present work is a fractional-step method using the collocated grid on a general curvilinear coordinates as described in Nakayama and Sakio (6). Details are summarized in Table 1. First the equations of motion are integrated in time by Adams-Bashforth scheme by differencing the viscous and SGS terms using the second-order central difference scheme and the convective terms by a second-order conservative difference scheme. The boundary condition for the cells next to the bottom boundary is that the wall shear stress is set by the wall model. Then the pressure is computed by solving the Poisson equation to satisfy the continuity equation and the velocity is also corrected.

Table 1 Summary of numerical calculation method

Model elements	Method
Coordinates	Sigma-coordinate system
Grid	Collocate
Calculation algorithm	Fractional-step method
Convective term	Second-order conservative central difference
Viscous term	Second-order central difference
Pressure solution	SOR method
Time marching method	Second-order Adams-Bashforth method

CALCULATION AND RESULTS

The wall model described above has been tested in two test flows, both of which involve curved surfaces with flow separation. The combination of models tested are summarized in Table 2. The first test case is a fully-developed closed-channel flow with hill-like obstacles on the bottom surface as shown in Fig. 1. The second case is a fully-developed open-channel flow over wavy bed shown in Fig. 5. For both of these flows the bottom boundary is curved and the equations are first transformed onto a curvilinear coordinate system before being numerically solved in the same way as was done in the DNS (6). The results are presented in the rectangular coordinates (x,y,z), the streamwise, vertical and spanwise distances with corresponding velocity components (u,v,w), with the notation for the average and the filter as defined before.

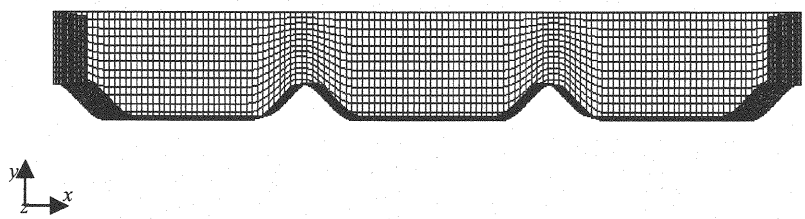

Fig. 1 Computational grid for flow past periodic train of model hills

Table 2 Summary of numerical calculation method

abbreviation	SGS model	Wall model
SdS+LL	Standard Smagorinsky model	Log law
SdS+WW	Standard Smagorinsky model	Power law by Werner and Wengle
SdS+WSM	Standard Smagorinsky model	Wall stress model
SdS+NS	Standard Smagorinsky model	No-slip
SIS+LL	Shear-Improved Smagorinsky model	Log law
SIS+WW	Shear-Improved Smagorinsky model	Power law by Werner and Wengle
SIS+WSM	Shear-Improved Smagorinsky model	Wall stress model
SIS+NS	Shear-Improved Smagorinsky model	No-slip

Flow over train of model hills

The first test case is the flow in a closed channel with hill-like obstacles placed on the bottom surface at a constant interval defined by Almeida et al. (14) and a well-resolved accurate LES calculation of this flow has been done by Temmerman and Leschziner (5). The numerical grid used to compute this flow is shown in Fig.1. The hill-like obstacles of height h are placed at a constant pitch of $9h$ in a duct of height $3.035h$. The upper boundary is a no-slip wall and the flow is fully developed, the computation can be done assuming the flow extends periodically in the streamwise and the lateral directions. The computational region contains three hills as shown in the figure and its dimensions are $9h$x$3.035h$x$4.5h$ in the streamwise, vertical and the lateral directions covered by the computational grids of 60x18x30. As can be seen from Fig. 1, the grid spacing is taken large enough so as not to resolve the wall region deliberately for the purpose of testing the wall model to be used in a high-Reynolds number simulation. The first point from the bottom bed is more than 30 wall units away.

Calculations were done for a Reynolds number based on h and U_b, the average velocity in the cross section containing the top of the hill, of 10595 which is the same as the value used by Temmerman and Leschziner (5). The results of calculations for this flow at three streamwise locations are shown in Figs. 2 through 4. The three locations are, a section on the down-slope lee side of the hill where the flow is separated, the middle of the flat bottom section which is just downstream of the reattachment point and on the upslope side of the next hill where the flow is accelerated. Each figure has two plots, one for the results of four different wall models including the case with no wall-model combined with the standard Smagorinsky model (SdS) for the SGS stress and the other one for similar results obtained with shear-improved Smagorinsky model (SIS). The solid line denotes the results of the well-resolved LES which can be regarded as the reference. From the plots of the mean velocity profile results, one can see that all wall models do fairly well on the accelerating up-slope position. The results in the re-circulating region and downstream of reattachment obtained with the LL and WW models with either SdS or SIS are grossly deviated from the well-resolved LES. The results obtained by the presently proposed wall stress model (WSM) agree consistently well with the well-resolved LES with either SdS or SIS model. It should also be noted that the SdS and the no wall model (SdS+NS) combination is not too far off the well-resolved LES. It is thought that a combination of underestimated velocity gradient near wall and over-estimated eddy viscosity may have cancelling effects. SdS+WSM and SIS+WSM results are similar. The reason for this is that the SIS model is different from SdS model only in the near wall region. Therefore, if the wall stress is equal, SdS and SIS results are similar.

Fig. 3 shows the similar results of the Reynolds shear stress $-\overline{u'v'}$ where the primes indicate the deviation of the instantaneous velocity from its time mean and the contribution from the modelled part of the stress is included. The results of LL and WW are seen to be very close and generally under-predict $-\overline{u'v'}$. The WW model after all is a minor refinement of the LL. Remarkably, the no wall model NS does fairly well when used with SdS but not with SIS. The SIS model, which was shown to do well in homogeneous turbulent flow and wall-bounded turbulent shear flow, but has not been tested in a separated shear layer like the present flow appears to over-damp the eddy viscosity and give too little Reynolds stresses.

Fig. 4 shows similar results for the streamwise normal stress $\overline{u'u'}$. The same trend seen with the shear stress shown

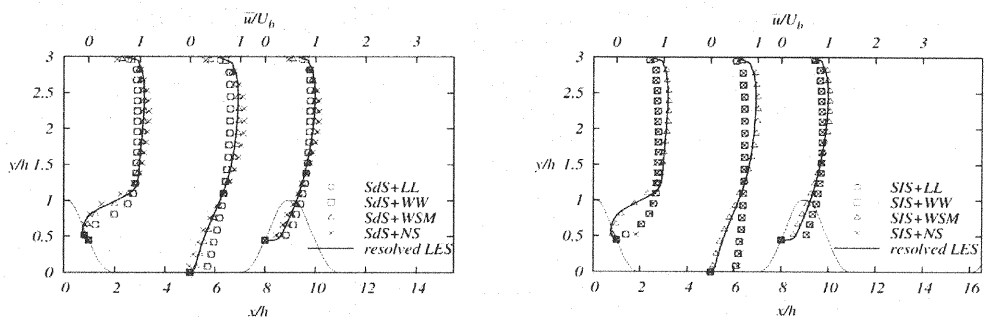

(a) SdS model (b) SIS model

Fig. 2 Streamwise mean velocity results using the Standard Smagrinsky (SdS) model and the shear-improved Smagorinsky (SIS) model

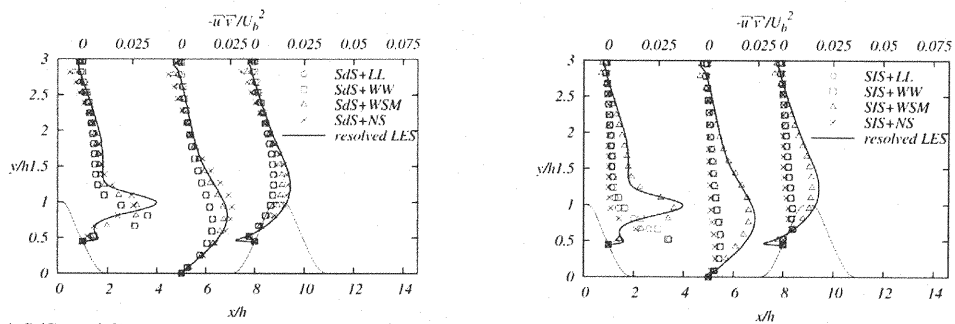

(a) SdS model (b) SIS model

Fig. 3 Reynolds shear stress results using the Standard Smagrinsky (SdS) model and shear-improved Smagorinsky (SIS) model

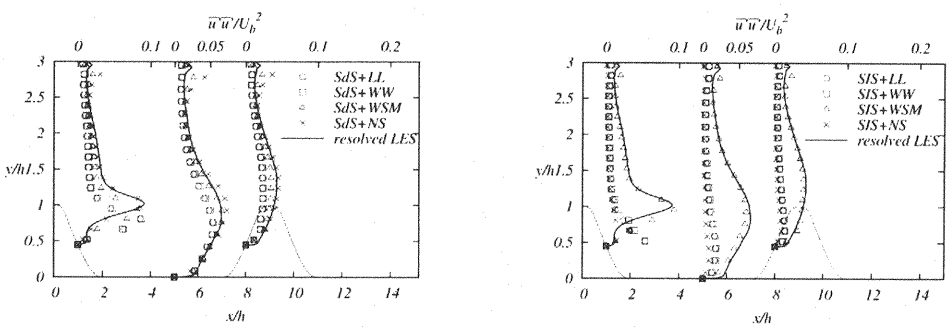

(a) SdS model (b) SIS model

Fig. 4 Streamwise Reynolds normal stress results using the Standard Smagrinsky (SdS) model and shear-improved Smagorinsky (SIS) model

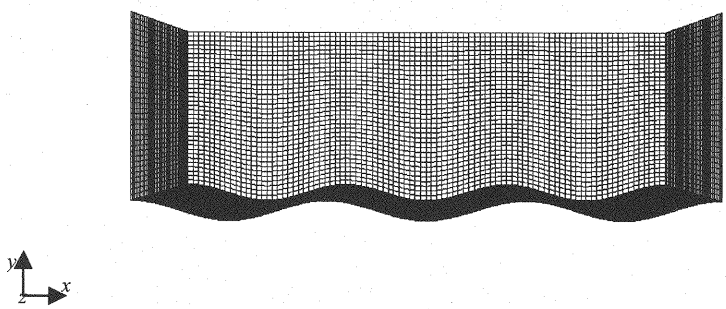

Fig. 5 Calculation grid for flow over wavy bed.

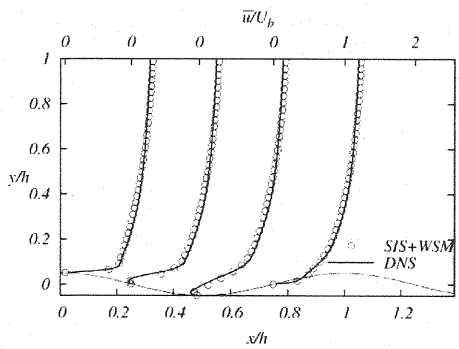

Fig. 6 Streamwise mean velocity

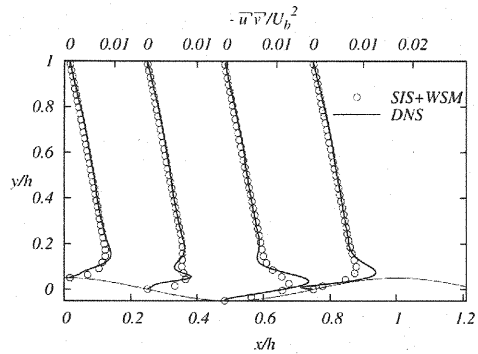

Fig. 7 Reynolds shear stress

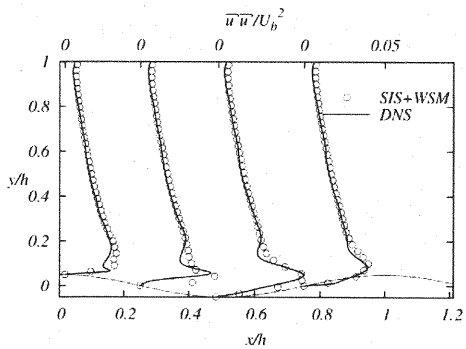

Fig. 8 Streamwise Reynolds normal stress

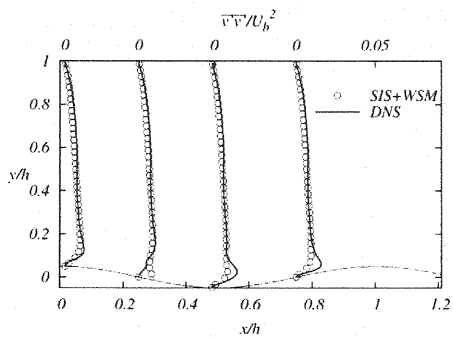

Fig. 9 Vertical Reynolds normal stress

in Fig. 3 is also seen here, which confirms that the WSM does predict the normal stress well.

The second test case is an open-channel flow with a wavy bed for which there are DNS data though the Reynolds number is smaller. The Reynolds number based on the average channel depth and the average velocity is 6760 (6). The channel bed consists of sinusoidal waves with amplitude 5% of the channel height and the wave length is equal to the depth as shown in Fig. 5. The maximum slope is steep enough for the flow to separate at the lee side of the waves. The upper boundary is treated as a fixed flat free-slip surface. The number of grid points used in the present LES calculation is 90x35x48 which is less than 1/3 of the DNS in all directions. The grid spacing in the vertical direction is made constant as seen in Fig. 5. The vertical spacing in wall units is about 25 and the wall layer is not revolved. Calculation for this case is done with the combination (WSM+SIS) of the wall and SGS models that was found to do best in the first test case.

The results of the mean velocity profiles, the Reynolds shear stress, the streamwise normal stress and the vertical normal stress components at the top of the waviness, halfway to the bottom, at the bottom and half way to the next peak are shown in Figs 6 through 9. Mean velocity distributions are seen to agree very well with the DNS results. The Reynolds

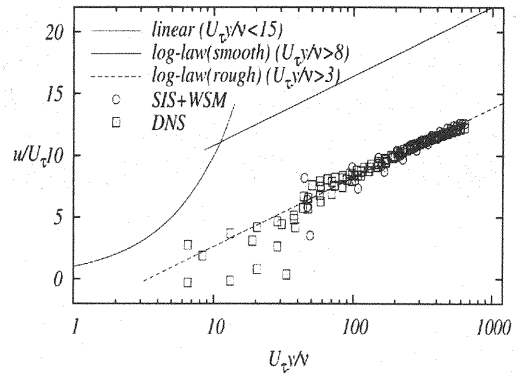

Fig. 10 Mean velocity profiles plotted in the wall coordinates based on overall resistance

stress results are seen to agree fairly well with the DNS results except the peaks in the stress distributions near the edge of the separated region downstream of the waviness peak are milder than the DNS. These LES results do not contain the sub-grid contributions and must naturally be smoother than the actual.

The waviness in the present test flow may be regarded as roughness placed over flat surface. In fact the flow about four roughness heights (peak-to-peak amplitude in the present sinusoidal surface) above the mean wall position is not directly influenced by the details of the waviness (6) and the mean velocity distribution follows the logarithmic profile for rough surfaces. The friction velocity in this case is deduced from the overall pressure gradient and not the local viscous stress or its average. Fig. 10 is a plot of the mean velocity profiles at four streamwise locations same as those shown in Fig. 6, normalized by the friction velocity U_τ that is calculated from the applied pressure difference Δp over the length of the channel L, $\sqrt{h\Delta p/\rho L}$ plotted against $U_\tau y/\nu$ in semi-log scale. one can see that the velocity profile in $U_\tau y/\nu>100$ lies nearly on a straight line that is parallel to the logarithmic law for smooth surface shifted down by about 8 U_τ. The roughness function ΔU^+ for sand-grain roughness of height same as the peak-to-peak height of the present sinusoidal roughness is about 4 (Schlichting (15), Colebrook (16)). Buckles et al. (17) found experimentally that the equivalent roughness height of a sinusoidally wavy surface is about twice the peak-to-peak amplitude and the present LES results agree well with it.

CONCLUSIONS

A simple wall stress model based on a surface resistance formula has been proposed and tested in the calculation of turbulent flows in channels with hill-shaped obstacles and a wavy bottom bed. The subgrid-scale stresses are modelled with commonly used standard Smagrinsky and the shear-improved Smagorinsky subgrid-scale models. The results of the mean velocity and the turbulent stresses are evaluated by comparing them with the well-resolved LES and DNS results. The proposed model is shown to perform consistently better than the commonly used algebraic models based on the log-law, and power-law similarity in flows over complex geometry that induces flow separation and reattachment. The model coefficient is determined by using a resistance formula for flat surface in terms of the bulk flow parameters which assures the overall resistance is calculated correctly. It can also be used for calculating of practical flows over complex and rough surfaces.

REFERENCES

1. Sagaut, P. : Large Eddy Simulation for Incompressible Flows, 3rd ed., Springer-Verlag, Berlin Heidelberg, 2006.
2. Grinstein, F., Margolin, L.G. and Rider, W. J. : Implicit Large Eddy Simulation, Cambridge University Press, 2007.
3. Piomelli, U. and Balaras,E.: Wall-layer models for large-eddy simulations, Annu. Rev. Fluid Mech, Vol.34, pp.349-374, 2002.
4. Kitano,Y. and Nakayama,A.. : Large-Eddy Simulation of High Reynolds Number Channel Flow Applying Explicit Filtering, Annual Journal of Hydraulic Engineering, Vol.53, pp.1021-1026, 2008 (in Japanese).
5. Temmerman, L. and Leschziner, M.A.: Large Eddy Simulation of separated flow in a streamwise periodic channel construction, Proc. 4th. Int. Symp. on Turbulence and Shear Flow Phenomena, Stockholm, pp.27-29, 2001.
6. Nakayama, A. and Sakio, K. :Direct Numerical Simulation of Turbulent Flow Over Complex Wavy Rough Surface, Journal of Applied Mechanics JSCE, Vol.11, pp.839-846, 2003(in Japanese).
7. Kline, M.: An attempt to assess the quality of large eddy simulations in the context of implicit filtering, Flow,

Turbulence and Combustion, Vol.75, pp.131-147, 2005.
8. Smagorinsky, J. : General circulation experiments with the primitive equations. I. The basic experiment, Mon. Weather Rev., Vol.91, pp.99-164,1963.
9. Leveque, E., Toschi, F., Shao, L. and Bertoglio, J. P.: Shear- improved Smagorinsky model for large-eddy simulation of wall- bounded turbulent fows, J. Fluid Mech., Vol.570, pp.491-502, 2007.
10. Nakayama, A, Noda, H. and Maeda, K. : Similarity of instantaneous and filtered velocity fields in the near wall region of zero-pressure gradient boundary layer, Fluid Dynamics Research, Vol.35, No.4, pp.299-321, 2004.
11. Vengadesan, S. N. and Nakayama, A : Large eddy simulation of flow over smooth hill using one-equation subgrid scale model, Proc. 2000 Meeting of Japan Society of Fluid Mechanics, pp.595-596,2000.
12. Schoenherr, K. E. : Resistance of at surfaces moving through a fluid, Trans.SNAME,Vol.40, pp.279-313, 1932.
13. Werner, H. and Wengle, H. : Large-eddy simulation of turbulent flow over and around a cube in a plate channel, Proc. 8th Symp. On Turbulent Shear Flows, Munich, Germany, pp.1941-1945, 1991.
14. Almeida, G. P., Durao, D.F.G. and Heitor, M.V.: Wake flows behind two dimensional model hills, Exp. Thermal and Fluid Science, Vol.7, pp.87-93, 1992.
15. Schlichting, H. : Boundary-Layer Theory, 7th ed. McGraw-Hill, New York, 1979.
16. Colebrook, C.F. : Turbulent flow in pipes with particular reference to the transition between smooth and rough pipe laws, J. Inst. Civ. Eng., Vol.11, pp.133-156,1939.
17. Buckles, J., Hanratty, T. J. and Adrian, R. J. : Turbulent flow over large-amplitude wavy surfaces, J. Fluid Mech., Vol.140, pp.27-44,1984.

APPENDIX - NOTATION

The following symbols are used in this paper;

A =constant in the log law;
B = constant in wall stress model;
C_d =resistance coefficient;
Cs =Smagorinsky constant;
g_i =components of gravitational acceleration;
h =hill height;
P = pressure;
S =rate of deformation tensor;
t = time;
u', v' = fluctuating velocity components in x and y directions;
u_i = Cartesian velocity components;
u_1 =streamwise velocity at the point closest to the wall;
$\overline{u}$ =mean streamwise velocity;
U_0 =cross-sectional mean velocity
U_τ =mean friction velocity
x =streamwise coordinate;
x_i =rectangular coordinate;
y =virtical coordinate;
$y+$ =wall distance;
Δ =the geometric average of grid spacing in three directions;
Δ_x =grid spacing in the streamwise direction;
κ = von Karman constant (= 0.41);
ν =kinematic viscosity coefficient;
ν_t =kinematic eddy viscosity coefficient;
ρ =fluid density;
τ_{ij} =sub grid scale stress;
τ_w =wall shear stress;
$\bar{}$ =ensemble or time average;

(Received Aug 03, 2009 ; revised Jan 29, 2010)